Vol. 46 No. 1 SCIENCE IN CHINA (Series E) February 2003

Synthesis process and growth mechanism of g′-Fe_4N nanoparticles by phase-transformation

CAO Maosheng (曹茂盛)[1,2], LIU Haitao (刘海涛)[1], CHEN Yujin (陈玉金)[1],
WANG Biao (王 彪)[3] & ZHU Jing (朱 静)[2]

1 Department of Material Science and Engineering, Harbin Engineering University, Harbin 150001, China;
2. School of Material Science and Engineering, Tsinghua University, Beijing 100084, China;
3 Center for Composite Materials, Harbin Institute of Technology, Harbin 150001, China
Correspondence should be addressed to Cao Maosheng(email:caomaosh@mail.tsinghua.edu.cn)

Received May 20, 2002

Abstract Multiphase Fe/N nanoparticles were synthesized by means of chemical vapor reaction, the influence of the preparing parameters on the properties of particles was studied carefully during the first nitriding process. The optimum process was determined. Single phase γ′-Fe_4N was prepared by twice-nitriding. Multiphase iron-nitride really transforms γ′-Fe_4N nanoparticle of single-phase and uniform. Moreover, the mechanism of nanoparticle nucleation and growth, including phase-transformation, was revealed. In addition, the mircograph, particle size, physical phases, schemical constituents and magnetic properties before and after phase-transformation were characterized initially.

Keywords: nanoparticles; surface reaction; phase-transformation; Iron nitride; *g* ′-Fe_4N

In 1984, Tanaka et al. synthesized sub-micron scale Fe/N particles with good magnetic characteristics ($s_s \approx 1\times10^5$ A·Wb^{-1}·Kg^{-1}, $H_C \approx 3.2\times10^4$ A·m^{-1})[1] by a one-step method of CVD. Since then a few groups have synthesized micron scale, sub-micron scale and nanometer scale nitride-iron particles by different synthesis routes[1—7]. In 1993, Nakatani et al. reported a new method for synthesizing *å*-Fe_3N magnetism grain with particle size less than 10 nm[2]. In 1999, Lee et al. reported the chemistry stability of the nitride-iron nanoparticles under atmosphere condition and the results showed that its anti-oxidization property was very bad if its surface was not pretreated[8]. However, the synthesis and magnetic properties of the single-phase nanoparticles such as *e*-Fe_3N and *g*′-Fe_4N have rarely been reported in literature.

From 1991 to 1995, research on the synthesis of magnetic nanoparticles, *e*-Fe_3N and *g*′-Fe_4N, was carried out in China by vapor method and vapor-liquid method with the particle sizes ranging from 10 to 50 nm, s_s 1.32×10^{5}A·Wb^{-1}·Kg^{-1} and H_C vlaue 3.5×10^4 A·m^{-1} [3—9]. In 1995, Liang et al. reported the experimental results of synthesizing nitride iron nanoparticles by the laser inducing Fe $(CO)_5$, and the products were *g*′-Fe_4N and *e*-Fe_3N compounds with sizes from 10 to 25 nm, the H_C value 4.0×10^4 A·m^{-1} and the σ_s value 5.86×10^4 A·Wb^{-1}·Kg^{-1} [3]. In 2000, Guo et al. prepared of magnetic liquid nitride iron by vapor-liquid method with liquid phase as carrier and

e-Fe_3N as the main phase. The products still had impurities such as z-Fe_2N, g'-Fe_4N, α-Fe and Fe_3O_4. At the same time, Liu S et al. reported the synthetic process of needle-like ultra-fine magnetic powder g'-Fe_4N with average size 82.9 nm, the H_C value $4.46\times10^4\,A\cdot m^{-1}$ and the s_s value $1.33\times10^5 A\cdot Wb^{-1}\cdot Kg^{-1}$ [10]. In 2001, we synthesized the single-phase spheroid magnetic particles g'-Fe_4N with the average size smaller than 50 nm by the second nitriding method[11].

Up to now compounds of nitride-iron with wider range chemical ratio such as z-Fe_2N, e-Fe_3N, g'-Fe_4N, and $Fe_{16}N_2$ have already been obtained. Nitride-iron nanoparticles synthesized by means of vapor method and vapor-liquid method are all multiple-phase particles[12]. In the present work, Fe/N multiple-phase nanoparticles were synthesized by means of vapor method, and the g'-Fe_4N nanoparticles towards spherical chain shape were prepared through phase-transformation. The nitriding process has been studied carefully and the optimum process has been given. Especially, the properties of nanoparticles before and after phase-transformation have been characterized initially. In addition, the influence of synthetic parameters on the productivity and properties of nanoparticles g'-Fe_4N has been illuminated in detail.

1 Synthesis system and reaction process

1.1 Synthesis system

The synthesis system for the multiphase Fe/N nanoparticles consists of a reactive gas evaporing zone, reactive gas preheating zone, gas mixing zone, nucleation zone, growth zone, etc. The reactive gas, protective gas and carrier gas must be mixed up uniformly before reaction; uniform nucleation must be realized in the reaction zone; the particles should grow uniformly in the growth zone. Uniform mixing of reaction gas, nucleation and growth in coaxial heating zone were realized in our work, therefore overcoming the shortcomings of the original reactor. Here, the reaction gas, protective gas and carrier gas were mixed up uniformly by a mixing even apparatus, and then sent to the reaction zone. In the reaction zone, reaction started as soon as the reaction gas and protective gas got mixed. The particle nuclei were carried away from the reaction zone with the fluid of carrier gas. In the coaxial heating zone, the nuclei grew evenly and flowed into the collection zone under the condition of negative pressure.

1.2 Reaction process

The reaction raw materials should be pretreated to remove such impurities as water in ammonia, hydrogen and bichloride iron powder before the experiment. After this process, the vapor chemical reaction was carried out at high temperature between metallic halide and reducing gases such as ammonia and hydrogen to accomplish the first nitriding. The products were composed of nitride, iron, unreacted metallic halide and the by-product ammonium chloride. The second nitriding process of nitride-iron particles should be done via phase-transformation at lower temperature in order to obtain the uniform single-phase g'-Fe_4N nanoparticles. The final product was uniform, highly pure, sphere-shaped, single phase, ultra-fine and highly magnetic g'-Fe_4N particles.

2 Synthetic parameters

2.1 Pretreatment parameters of raw materials

Crystalline water in the $FeCl_2.nH_2O$ should be removed because it is disadvantageous to the synthesis of nitride-iron. This experiment adopted the dry process to dehydrate $FeCl_2.nH_2O$, and used nitrogen as protective gas to prevent $FeCl_2.nH_2O$ from oxidizing and dehydrating. Here, the suitable dehydration parameters such as dehydration temperature, pressure and time were defined by repeated experiments. The dehydration temperature, dehydration pressure and dehydration time were 230℃, 0.81×10^5 Pa and 30 min, respectively. After dehydration DTA measurement was made for the $FeCl_2$ powder and the result showed that the evaporation velocity was related to evaporation temperature, evaporation pressure and evaporation time. Therefore, we investigated the relation between the evaporation quantity and the three parameters. The evaporation temperature, evaporation pressure and evaporation time we determined in experiment were 750℃, 0.81×10^5 Pa and 25 min, respectively.

2.2 Process parameters

Our experiments have proved that there are parameters affecting phase composition and productivity, such as reaction pressure, reaction temperature, and ratio of reacting gases. In the experiment, the relations between the parameters and product properties such as reaction temperature and phase composition, reaction temperature and the productivity, reaction temperature and the particle size and range, reaction temperature and the magnetic properties, were examined (table 1 and figs. 1—4). Obviously, the appropriate reaction temperature range was 850—950℃. In order to search for a better reaction pressure, at certain temperature, the relations between the pressure and productivity, and the relations between the pressure and size of the particles were studied carefully. The results are shown in figs. 5 and 6. Obviously, the pressure should be controlled within 0.71×10^5—0.91×10^5 Pa. The theories and experiments all confirmed that both nucleation velocity and the growth velocity were the function of the partial pressure of gas at given temperature. The size of iron-nitride depended on the partial pressure of NH_3, H_2 and N_2 at certain temperature of the evaporation cell and total flow for given partial pressure of Fe_2Cl gas. Experiments gave the dependence of phase composition and productivity on the ratios of the raw gas to the reaction gas (the mol-ratios of $FeCl_2$ and NH_3) as well as the dependence of the relative content of the nitrogen in the products on the ratios of the reduced gases, i.e. the volume ratio of

Table 1 The relation between temperature and state phase

The reaction temperature/℃	780	880	980
Phase composition	e-$Fe_{2\text{-}3}N$ a-Fe	e-$Fe_{2\text{-}3}N$ g'-Fe_4N a-Fe	g'-Fe_4N g'-Fe

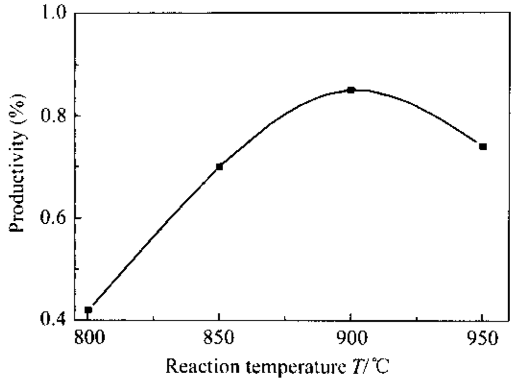

Fig. 1. The relation between temperature and productivity of particles. $P=0.71\times10^5$ Pa; $t=60$ min

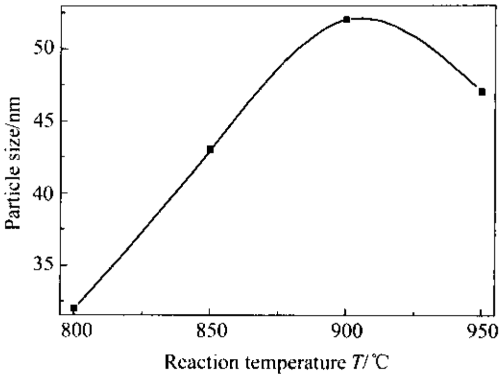

Fig. 2 The relation between temperature and size of particles. $P=0.71\times10^5$ Pa; $t=60$ min.

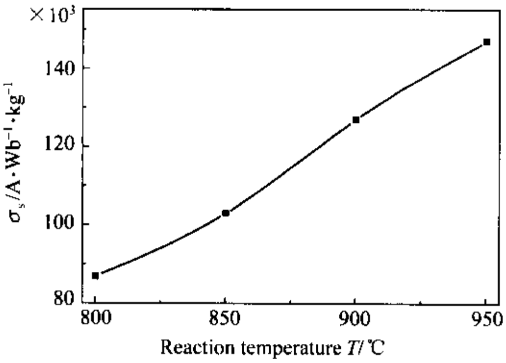

Fig. 3. The relation between the temperature and s_s of the particles. $P=0.81\times10^5$ Pa; $t=60$ min.

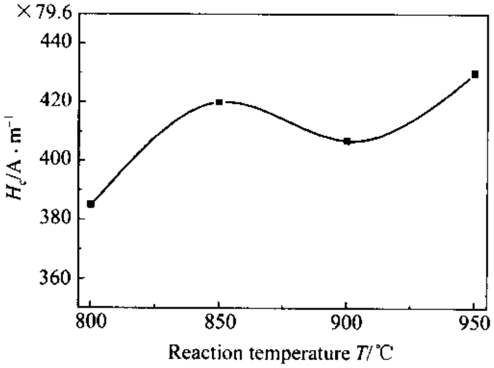

Fig. 4. The relation between the temperature and H_c of the particles. $P=0.81\times10^5$ Pa; $t=60$ min.

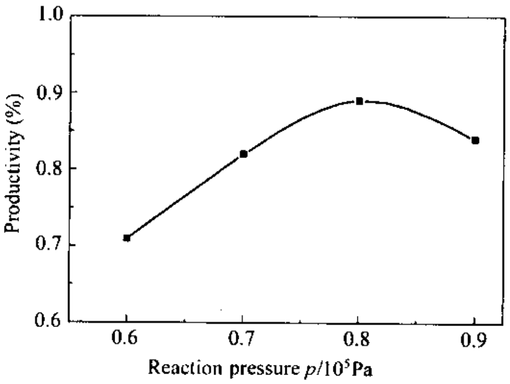

Fig. 5. The relation between pressure and productivity of particles. $T=900$℃; $t=60$ min.

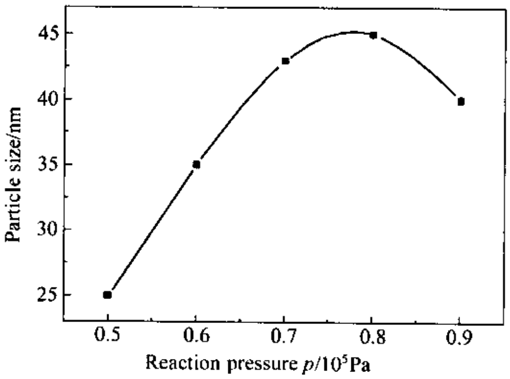

Fig. 6. The relation between pressure and diameter of particles. $T=900$℃; $t=60$ min.

NH_3 to H_2 (table 2, figs. 7 and 8). The ratio of the raw gas to the reaction gas should be above 35 and the ratio of the reducing gases above 1.5.

Table 2 The relation between raw gas and state phase

$NH_3/FeCl_2$ (vol-%)	40	35	30	20
Phase composition	e-$Fe_{2\text{-}3}N$ g'-Fe_4N	e-$Fe_{2\text{-}3}N$, g'-Fe_4N, a-Fe	e-$Fe_{2\text{-}3}N$ e-Fe	e-Fe Fe_3O_4

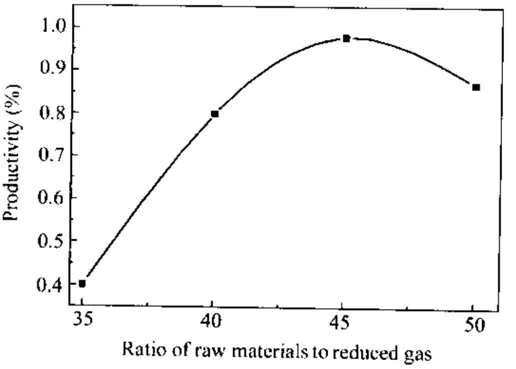

Fig. 7. The relation between productivity and ratio of $FeCl_2/NH_3$. T=900℃; $p=0.71\times10^5$ Pa; t=60 min.

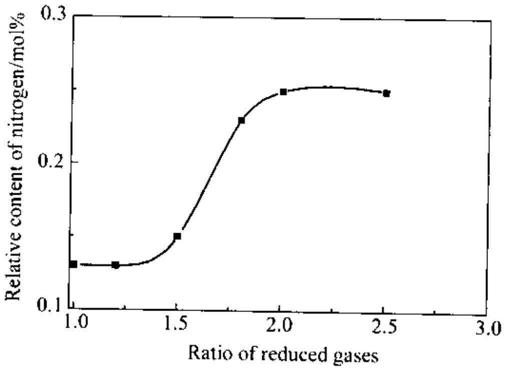

Fig. 8. The relation between relative concentration of N and ratio of NH_3/H_2. T=900℃; $p=0.71\times10^5$ Pa; t=60 min.

By probable reaction and the theory of UFP nucleation growth, we can realize the second nitriding using the particles prepared by the first nitriding to make the Fe/N change into g'-Fe_4N. The results of our experiments proved that the appropriate values of temperature, pressure and time for twice-nitriding are 350℃—450℃, 1.0×10^5 Pa, 30—60 min, respectively. Obviously, the twice-nitriding temperature is much lower than those of micron-scale iron or Fe/N. The reason is just that nanoparticles generally have higher reaction activity than that of microparticles.

3 Model of nucleation and phase-transformation

3.1 Thermodynamics and kinetics for particle nucleation

Based on nucleation thermodynamics and reaction balance constant, particle formation depends on the ratio between nucleation and nuclei growth. Here, R_n and R_s stand for nucleation velocity and growth velocity, respectively. Hence the synthesis process can be expressed as

$$Fe_xN\ (g) \xrightarrow{R_n} Fe_xN(\text{crystal nuclei}) \xrightarrow{R_s} Fe_xN\ (\text{UFP}), \tag{1}$$

where nucleation velocity may be written as

$$R_n = A\exp[-16\eth s^3V^3/3kT(kT\ln p/p_0)^2]. \tag{2}$$

In formula (2), A is a constant, and k is Boltsmann constant, T is temperature, V is molecular volume, p and p_0 respectively stand for vapor pressure and balance pressure on micron-nuclei surface, and p/p_0 is the ratio of oversaturation. Obviously, larger p/p_0 is benefit to nucleation. The radius of critical crystal nuclei can be expressed as

$$r = (2sV)/[kT\ln(p/p_0)]. \tag{3}$$

From formula (3), larger p/p_0 helps to reduce the radius of critical crystal nuclei. At the same time, larger p/p_0 helps to increase UFP productivity. On the other hand, the particle diameter after nucleation is often determined by

$$d = A\left(h C_0 / N\right)^{1/2}, \tag{4}$$

where A is a constant; h is reaction degree of conversion; C_0 is reactant concentration; N is the mol number of reactant-product particles in unit volume. It can be seen that larger p/p_0 value results in higher R_n at the initial period, while the reduction in p/p_0 may lead to a decrease in R_n and an increase in R_s. Therefore the particles should be removed from reaction cell as quickly as possible to restrict particle growth.

Here we should point out that initial particle sizes in synthesis process are several nanometers and they are often in suspended state. Therefore, Brown motion law can describe their motions at this moment. Obviously, the interactions among particles will result in particle condensation. According to gas-molecular kinetics, collision frequency can be written as

$$f = 4(\eth kT / m)^{1/2} d_p N^2, \tag{5}$$

where N is particle concentration, *m is* particle mass, d_p is particle diameter, and k is Boltsmann constant. The retention time of particles must be controlled effectively and the initial concentration of particles must be reduced in order to limit particle growth due to collision and agglomeration. In other words, the produced particles have also to be removed from the reaction cell.

3.2 Growth and aggregation after nucleation

One single nucleus in vapor growth is generally relevant to the growth conditions and its environments. Suppose that there is neither reaction growth nor monomer adsorption in single nuclei, nor adsorption reaction between particles and reactant or intermediate. Then the growth velocity of single nuclei can be described by means of Tamman model under the condition of sharp-cooling. In this situation, the temperature corresponding to the fastest nucleation velocity is much lower than that of growth velocity. Therefore, if particles are cooled down rapidly, the particle growth can be confined without affecting the nucleation rate. In fact, the mechanism mentioned above is very popular in fast phase change. It is just the theoretical basis for synthesizing UFP by chemical vapor reaction.

3.3 Phase-transformation process and twice-growth

According to the one-step-synthesis products, we can predict that there exist several chemical reactions in twice-nitriding process[7,13], and their reaction formulas are as follows:.

$$4Fe\ (s) + 2NH_3 \xrightarrow{350\sim450} 2Fe_2N\ (\text{Particle}) + 3H_2 \tag{6}$$

$$8Fe\ (s) + 2NH_3 \xrightarrow{450} 2Fe_4N(\text{Particle}) + 3H_2 \tag{7}$$

$$4Fe_2N\ (s) \xrightarrow{450} 2Fe_4N(\text{Particle}) + N_2 \tag{8}$$

$$8\ Fe_3N\ (s) \xrightarrow{450} 6Fe_4N(\text{Particle}) + N_2 \tag{9}$$

Here, extension growth and surface reaction growth are two important characteristics of particle growth in phase-transformation. It is an obvious phenomenon of original nuclei growth, which is relevant to two mechanisms of surface reaction and surface diffusion owing to adsorption among nuclei and adsorption between nuclei and intermediate. In a general nucleation process, fresh nucleous surface will adsorb atoms or ions in reactant, and there occurs corresponding chemical reaction in particle surface. Both extension growth and surface reaction growth will result in particle surface expansion. The growth temperature and component of different atoms affect particle growth velocity. This is very important in synthesizing UFP with high chemical-ratio precision.

4 Characterization of the particle g'-Fe$_4$N before and after phase-transformation

The micrographs of nanoparticles before and after transformation are observed by means of SEM (fig. 9(a) and (b)). Fig. 9 shows that the Fe/N particles of the first-nitriding is spherical in shape, while the particles of the second-nitriding are spherical chain-shaped. The particle size is calculated by SEM and XRD; their corresponding sizes are shown in fig. 10 (a) and 10(b). The first nitriding ranges from 5 to 20 nm with the average size of 10 nm, and the second nitriding from 20 to 80 nm with the average size 50 nm. We can arrive at a conclusion that the particles size grows distinctly due to phase-transformation during the second-nitriding. Moreover, there exist the phenomena of the particle growth and slight agglomeration in the process.

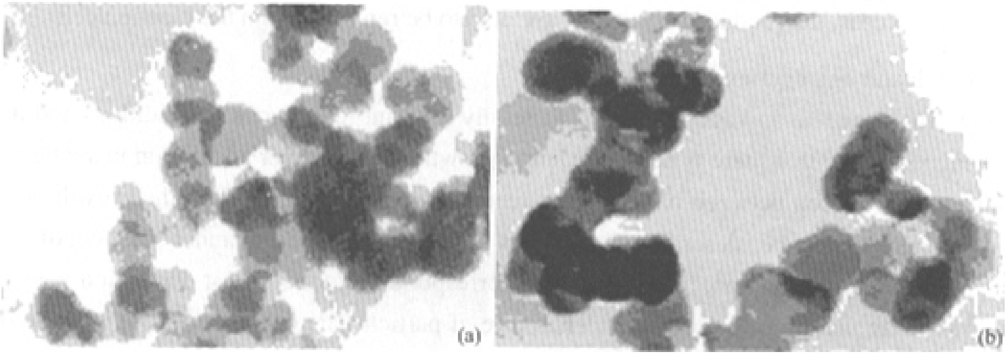

Fig. 9. TEM photograph of nanoparticles. (a) Before phase-transformation; (b) after phase-transformation.

Fig. 11(a) shows the XRD patterns of the particles obtained by the first nitriding. Checking the standard cards, we see that the particles contain s-Fe, e-Fe$_{2\text{-}3}$N, g'-Fe$_4$N, FeCl$_2$ and NH$_4$Cl. This reveals that the process of the first nitriding has a few sub-reactions, and therefore high pure g'-Fe$_4$N cannot be obtained. In fig. 11(b) are shown the XRD patterns of the particles after the second nitriding. There are four strong diffractive peaks in the figure which all are found to be the characteristic peaks of the g'-Fe$_4$N by checking the standard cards. Phase-transformations happens in the second nitriding process and the final product is the single-phase g'-Fe$_4$N with high phase contents. In oder to determine the chemical components of the particles after the first and the second nitriding, analyses were performed using an atomic absorption apparatus (WSY) and an element analytic apparatus (PE404C). The results are shown in table 3. Table 3 shows that

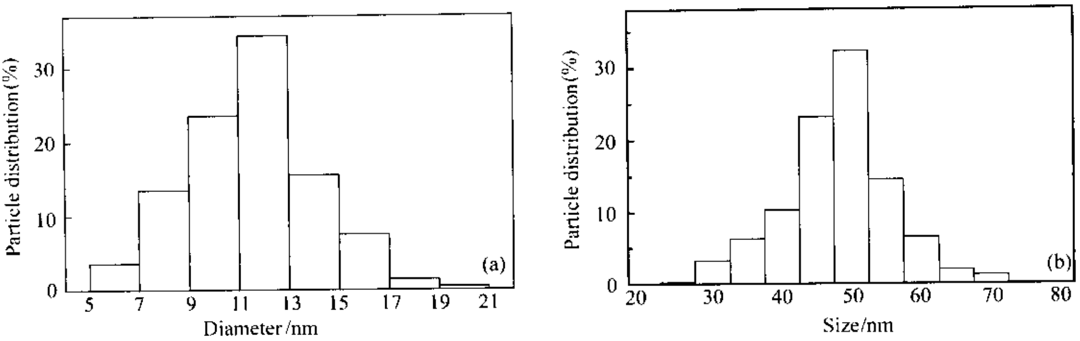

Fig. 10. The distribution of the particles diameter. (a) Before phase-transformation; (b) after phase-trans for mation.

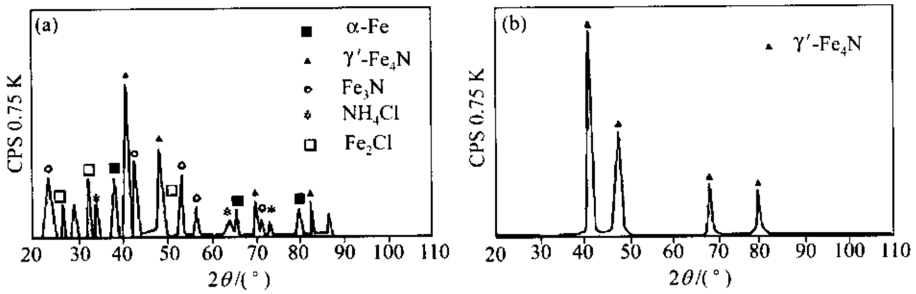

Fig. 11. XRD patterns of iron-nitride samples. (a) Before phase-transformation; (b) after phase-trans for mation.

there is no chlorine in the products after the second nitriding because Fe/N has been converted to single-phase *g* ′ -Fe$_4$N nanoparticles in the second-nitriding, and NH$_4$Cl is evaporated.

Table 3 Relative abundance of elements before and after transformation

Specimen	Fe	N	Cl	O	C
1	90.6	5.90	2.26	0.87	0.37
2	93.1	5.86	0	0.73	0.30

The magnetic properties of the particles are measured by means of VSM (table 4). The results indicate that specific saturated magnetic intensity and coercive force of nanoparticles *g* ′ -Fe$_4$N are higher than those of nanoparticles Fe/N. Obviously, the value of the specific saturated magnetic intensity in table 4 is also higher than that of refs. [1, 3], but is consistent with that of ref. [4].

Table 4 VSM measuring results of iron nitride nanoparticle

Magnetic properties	Before phase-transformation	After phase-transformation
σ_s/A · Wb^{-1} · Kg^{-1}	1.18×10^5	1.36×10^5
H_C/A · m^{-1}	1.78×10^4	3.72×10^4

5 Conclusions

A new synthetic process of uniform and single phase nanoparticles g'-Fe$_4$N has been put forth and the phase-transformation finished by twice nitriding technique. A series of experiments show that uniform, highly pure, spherically shaped single phase g'-Fe$_4$N could be obtained by twice nitriding, of which the particles size is less than 50 nm, the specific saturated magnetic intensity is 1.36×10^5A • Wb^{-1} • Kg^{-1} and the coercive force is 3.72×10^4 A • m^{-1}. The experimental results have proved that surface reaction and surface diffusion-growth in phase-transformation are the mechanisms of reaction and growth in the process of phase transformation.

Acknowledgements This work was supported by the China Funds of Excellent Youth and China Funds of Post Doctor, the National Natural Science Foundation of China and Post Doctor Funds of Heilongjiang Province.

References

1. Tanaka, T., Tagawa, K., Tasaki, A., Synthesis and some magnetic properties of iron nitride particles, J. Chem. Soc., 1984, (6): 930—934.
2. Nakatani, I. M., Iijikata, I., Ozawa, K., Iron-nitride magnetic fluids prepared by vapor-liquid reaction and their magnetic properties, Journal of Magnetism and Magnetic Materials, 1993, 122: 10—14.
3. Liang, Y., Zhao, X. Q., Zheng, F, et al., Magnetic properties of Fe-Nitride and cabo-nitride nanocrystalline particle, Metals Function Material, 1995, (4-5): 138—139.
4. Zhang, C. W., Huang, R. F., Yang. C. F. et al., Fe-N nanometer powder prepared by arc plasma reactive evaporation, Metals Function Material, 1995, (4-5): 139—141.
5. Cao, M. S., Deng, Q. G., Zhang. P. G., Preparing γ'-Fe$_4$N ultrafine powder by twice-nitriding method, Bulletin of the Chinese Ceramic Society, 1995, (6): 29—32.
6. Cao, M. S., Deng, Q. G., Synthesis of nitride-iron nano meter powder by thermal chemical vapor-phase reaction method, Journal of Inorganic Chemistry, 1996, 12(1): 88—91.
7. Cao, M. S., Science and Technology of the Ultra-fine Particle Preparation (in Chinese), Harbin: HIT Press, 1995, 131—136.
8. Lee, H. S., Nakatan. I., On chemical stability of iron-nitride magnetic fluids in atomospheric conditions, Journal of Magnetic and Magnetic Materials, 1999, 201: 23—26.
9. Guo, G. S., Wang, Z. H., Yu, S. et al., Preparation of iron-nitride magnetic fluid by vapor-liquid chemical reaction, Journal of Inorganic Materials, 2000,15(5): 921—925.
10. Liu, S. L, Teng, X. Y., Yu, Y. Y., Praparation and applications of magnetic fluid, Powder Metallurgy Industry, 2000, 10:(5): 32—39.
11. Cao, M. S., Wang, R. G., Fang, X. Y., Preparing g' -Fe$_4$N ultrafine powder by twice-nitriding method, Powder Technology, 2001, 115(1): 96—98.
12. Cao, H. M., Synthesis Handbook on Inorganic Compound (ed. the Chemistry Society of Japan) (in Chinese), Beijing: Chemical Industry Press, 1983, 444—445.
13. Cao, M. S, Xu, Q., Yang, L., Methodology on Synthesis and Preparation of Materials (in Chinese), Harbin: HIT Press, 2001, 11—12.